Available online at www.sciencedirect.com
SCIENCE DIRECT®
European Journal of Pharmacology 481 (2003) 41–50
www.elsevier.com/locate/ejphar

Antimigraine dotarizine blocks P/Q Ca^{2+} channels and exocytosis in a voltage-dependent manner in chromaffin cells

Ana Ruiz-Nuño[a,1], Inés Mayorgas[a,1], Jesús M. Hernández-Guijo[a,1], Román Olivares[a], Antonio G. García[a,b], Luis Gandía[a,*]

[a] *Departamento de Farmacología y Terapéutica, Facultad de Medicina, Instituto "Teófilo Hernando", Universidad Autónoma de Madrid, c/ Arzobispo Morcillo, 4, 28029 Madrid, Spain*

[b] *Servicio de Farmacología Clínica and Instituto de Gerontología, Hospital de la Princesa, Diego de León 62, 28006 Madrid, Spain*

Received 31 March 2003; received in revised form 4 September 2003; accepted 5 September 2003

Abstract

The mechanism of blockade of P/Q Ca^{2+} channels by antimigraine, dotarizine, was studied in voltage-clamped bovine adrenal chromaffin cells. Inward currents through P/Q channels were pharmacologically isolated by superfusing the cells with ω-conotoxin GVIA (1 μM) plus nifedipine (3 μM). Dotarizine (10–30 μM) blocked the P/Q fraction of I_{Ba} and promoted current inactivation. Thus, dotarizine caused a greater blockade of the late I_{Ba}, compared with blockade of the early peak I_{Ba}. This effect was more prominent, the longer was the duration of the depolarising pulse. The blockade of I_{Ba} was also greater at more depolarising holding potentials (i.e. −60 mV), than was the blockade produced at more hyperpolarising holding potentials (i.e. −80 or −110 mV). Catecholamine secretory responses to brief pulses (2 s) of a Krebs-HEPES solution containing 100 mM K^+ and 2 mM Ca^{2+} was blocked by 3 μM dotarizine. Blockade was faster and greater when dotarizine was applied on cells that were previously depolarised with Krebs-HEPES deprived of Ca^{2+} and containing increasing concentrations of K^+. This voltage-dependent blockade of P/Q channels and exocytosis might be the underlying mechanism explaining the dotarizine prophylaxis of migraine attacks.

Keywords: Dotarizine; Migraine; Ca^{2+} channels P/Q; Chromaffin cell; Catecholamine release

1. Introduction

Dotarizine (1-(diphenylmethyl)-4-[3-2(phenyl-1,3-dioxalan-2-yl-)-propyl]-piperazine), a novel piperazine derivative structurally related to flunarizine (Villarroya et al., 1995; Montiel et al., 1997; Novalbos et al., 1998, 1999), has shown clinical efficacy in the prophylaxis of migraine attacks (Galiano et al., 1993; Horga et al., 1996). Its antimigraine actions may be associated with its ability to block 5-HT receptors (Brasó et al., 1996; Montiel et al., 1997) and/or the blockade of voltage-dependent Ca^{2+} channels (Tejerina et al., 1993; Villarroya et al., 1995). In addition, dotarizine has been described as a "wide spectrum" Ca^{2+} channel blocker because it is able to completely block Ca^{2+} entry, $[Ca^{2+}]_i$ rise and secretion in bovine chromaffin cells, suggesting that it is capable of blocking the various Ca^{2+} channels subtypes in chromaffin cells (Villarroya et al., 1995; Lara et al., 1997).

Bovine chromaffin cells express L-, N- and P/Q-types of voltage-dependent Ca^{2+} channels. As much as 60% of the whole-cell current through Ca^{2+} channels is carried by P/Q channels (Albillos et al., 1996; Gandía et al., 1997); these channels are coupled to the K^+-evoked catecholamine release response more tightly than L- or N-channels (Lara et al., 1998). No study of the mechanism of Ca^{2+} channel current blockade elicited by dotarizine is available; hence, we thought it of interest to perform such a study on the P/Q component of the whole-cell Ca^{2+} channel current of bovine chromaffin cells, that can be pharmacologically isolated (Olivera et al., 1994; García et al., 2000). This study on P/Q channels is particularly relevant considering that these channels have been implicated in the pathogenesis of migraine (Ophoff et al., 1996).

* Corresponding author. Tel.: +34-91-397-53-96; fax: +34-91-397-53-80.
E-mail address: luis.gandia@uam.es (L. Gandía).
[1] These authors contributed equally to this work.

0014-2999/$ - see front matter © 2003 Elsevier B.V. All rights reserved.
doi:10.1016/j.ejphar.2003.09.013

2. Methods

2.1. Preparation and culture of bovine chromaffin cells

Bovine adrenal medullary chromaffin cells were isolated following standard methods (Livet, 1984) with some modifications (Moro et al., 1990). After isolation, cells were suspended in Dulbecco's modified Eagle's medium (DMEM) supplemented with 5% foetal calf serum, 10 μM cytosine arabinoside, 10 μM fluorodeoxyuridine, 50 IU ml^{-1} penicillin and 50 μg ml^{-1} streptomycin. For electrophysiological experiments, cells were plated on 1-cm diameter glass coverslips at a density of 5×10^4 cells per coverslip. For studies of catecholamine release, cells (5×10^6) were plated on 5-cm diameter plastic Petri dishes containing 5 ml of DMEM. The cells were used 1–4 days after plating.

2.2. Measurements of whole-cell currents through Ca^{2+} channels

Membrane currents were measured by means of the whole-cell configuration of the patch-clamp technique (Hamill et al., 1981). Coverslips containing the cells were placed in an experimental chamber mounted on the stage of a Nikon Diaphot inverted microscope. The chamber was continuously perfused at room temperature (22–25 °C) with a control Tyrode solution containing (in mM): NaCl 137, $MgCl_2$ 1, $CaCl_2$ 2, HEPES/NaOH 10, pH 7.4. For current recordings, 10 mM Ba^{2+} (instead of 2 mM Ca^{2+}) was used as the charge carrier, and 5 μM tetrodotoxin was added to suppress Na^+ currents. The cells were internally dialysed with a solution containing (in mM): NaCl 10, CsCl 100, tetraethylammonium.Cl 20, MgATP 5, EGTA 14, HEPES/CsOH 20, Na.GTP 0.3, pH 7.2.

Whole-cell recordings were made with fire-polished glass electrodes (resistance 2–5 MΩ) mounted on the headstage of a DAGAN 8900 patch-clamp amplifier, allowing cancellation of capacitative transients and compensation of series resistance. A Labmaster data acquisition and analysis board and an IBM-compatible computer with pCLAMP software (Axon Instruments, CA, USA) were used to acquire and analyse the data.

Unless indicated otherwise, the cells were clamped at − 80 mV holding potential. Step depolarisations to 0 mV from this holding potential lasted 50 ms and were applied at 10-s intervals, to minimize the rundown of Ca^{2+} currents (Fenwick et al., 1982). Cells with pronounced rundowns were discarded. Leak and capacitative currents were eliminated by using currents elicited by small hyperpolarising pulses.

External solutions were exchanged by a fast superfusion device consisting of a modified multi-barrelled pipette, the common outlet of which was positioned 50–100 μm from the cell. Control and test solutions were changed using miniature solenoid valves operated manually (The Lee, Westbrook, CT, USA). The flow rate (0.5–1 ml min^{-1}) was regulated by gravity to achieve a complete replacement of cell surroundings in less than 1 s.

2.3. Online measurement of catecholamine release

Bovine chromaffin cells (5×10^6) were introduced into a microchamber for cell superfusion at 37 °C, with a Krebs-HEPES solution of the following composition (in mM): NaCl 144, KCl 5.9, $MgCl_2$ 1.2, $CaCl_2$ 2, glucose 11, HEPES 10, pH 7.4. The superfusion rate was 2 ml min^{-1}. The liquid flowing from the superfusion chamber reached an electrochemical detector, model Metrohm CH9100 Hersau, that monitored "online" under the am-

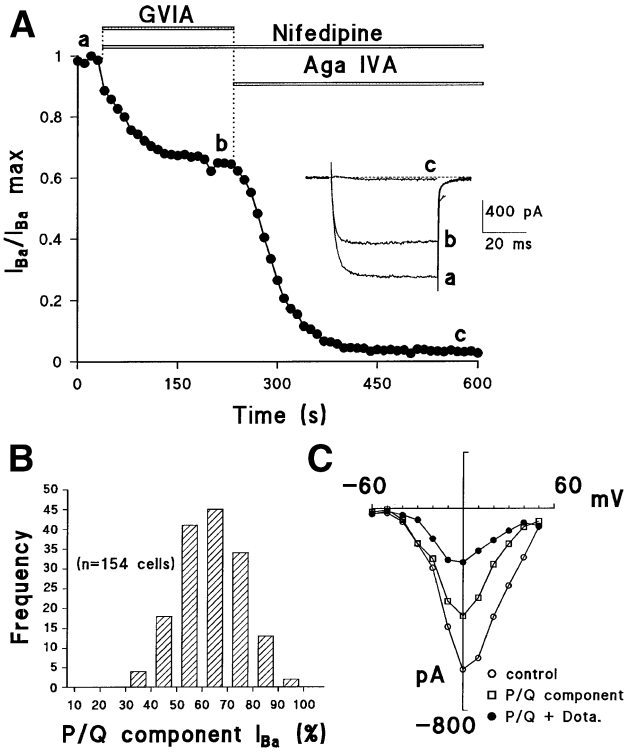

Fig. 1. Pharmacological dissection of non-P/Q and P/Q subcomponents of the whole-cell inward Ba^{2+} (10 mM Ba^{2+} was present in the extracellular solution) current through voltage-dependent Ca^{2+} channels expressed by bovine chromaffin cells. Panel A shows the time course of current blockade when the cell was initially superfused with a mixture of 1 μM ω-conotoxin GVIA (GVIA) and 3 μM nifedipine, and subsequently with 2 μM ω-agatoxin IVA (Aga IVA; in the absence of GVIA), during the time periods shown in the top horizontal bars. Normalised currents (I_{Ba}/I_{Ba}max) were plotted versus time. The inset shows original current traces from points a, b, and c of the time course curve. Panel B shows a frequency distribution histogram of the number of cells (ordinate) with a fraction of their whole-cell current carried through P/Q channels (abscissa). Panel C shows the relationship between voltage and current ($I-V$ curves) in a cell voltage-clamped at − 80 mV; test depolarising pulses at 10-mV steps were applied every 10 s. $I-V$ curves were performed before (control current), in the presence of 3 μM nifedipine and 1 μM ω-conotoxin GVIA (P/Q current), and in the presence of nifedipine, ω-conotoxin GVIA and 10 μM dotarizine (Dota).

perometric mode the amount of catecholamines secreted (Borges et al., 1986).

The cells were superfused continuously with a normal Krebs-HEPES solution containing 2 mM Ca^{2+}. At 2-min intervals, they were stimulated to secrete catecholamines with 2-s pulses of a K^+-enriched solution (100 mM K^+, 2 mM Ca^{2+}); the NaCl concentration of this solution was reduced on a molar basis to maintain isotonicity. The experimental protocols focused on studying the rate and extent of inhibition of the secretory response as well as the rate and extent of recovery after washout of the drug.

2.4. Materials and solutions

The following materials were used: collagenase from *Clostridium histolyticum* (Boehringer-Mannheim); bovine serum albumin fraction V, cytosine arabinoside, fluorodeoxyuridine and EGTA (Sigma); DMEM, foetal calf serum, penicillin and streptomycin (GIBCO); tetrodotoxin (Calbiochem). Dotarizine was obtained from Ferrer Internacional, Barcelona, Spain. All other chemicals were reagent grade.

Dotarizine was dissolved in dimethylsulphoxide (DMSO, Merck) at 10^{-2} M and diluted in saline solutions to the desired concentrations. At the highest concentrations used (no more than 0.1%), DMSO had no significant effects on I_{Ba}.

2.5. Statistical analysis

Data are expressed as means ± S.E.M. IC_{50} values were estimated by nonlinear regression analysis, using ISI software for a PC computer. Differences between nonpaired groups were compared by Student's *t*-test; a value of *p* equal or smaller than 0.05 was taken as the limit of statistical significance.

3. Results

3.1. Pharmacological dissection of P/Q channel current, from L and N currents

These experiments were done to establish the experimental conditions required to study the P/Q channel current in isolation, and the effects of dotarizine on this current. To determine the test potential that produced the maximum peak current, a current–voltage curve was performed at the beginning of each experiment. After the cytosol was reached with the patch pipette, the cell was voltage-clamped at − 80 mV and continuously fast superfused with an extracellular solution containing 10 mM Ba^{2+}. Fig. 1C shows an *I–V* curve for the current generated with 10-mV voltage steps. The threshold current was at − 40 mV, the current peaked at 0 mV (the current usually peaked at 0 to + 10 mV), and the reversal potential was reached close to + 60 mV. Thus, test pulses to + 10 mV, given at 10-s intervals, were used to study the time course of the effects of nifedipine, ω-conotoxin GVIA and ω-agatoxin IVA.

In the cell shown in Fig. 1A, test pulses to + 10 mV were continuously applied at 10-s intervals, from a holding potential of − 80 mV. The initial I_{Ba} stabilised at around − 1 nA. Superfusion with a mixture of nifedipine (3 μM) plus ω-conotoxin GVIA (1 μM) produced a progressive decline of the current amplitude that reached a new steady state at around − 0.55 nA in 2.6 min. Due to the irreversible

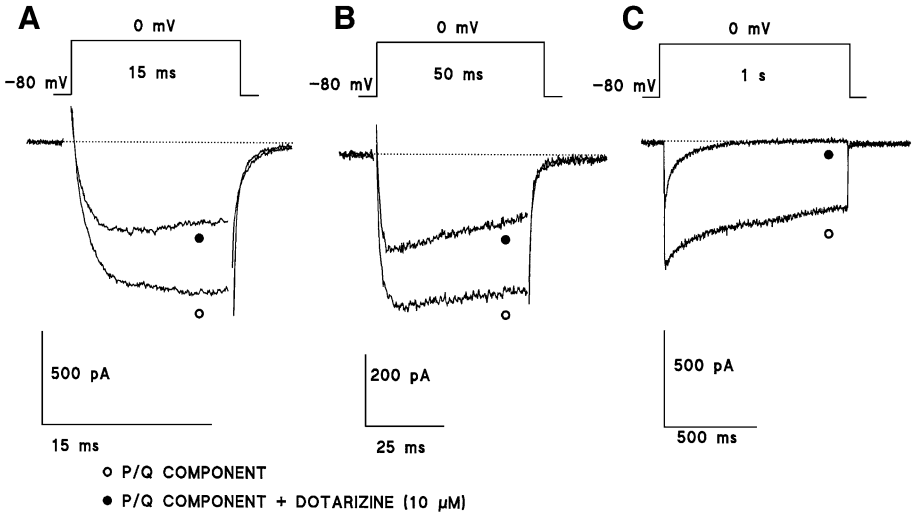

Fig. 2. Blockade of P/Q channel currents by dotarizine (10 μM), with depolarising test pulses of increasing duration. The holding potential was maintained at − 80 mV; test depolarising pulses to 0 mV were applied at 10-s intervals. In all cases, the cells were treated with L/N channel blockers, as in Fig. 1 (not shown). Three pairs of original current traces obtained in the absence and the presence of dotarizine in three different chromaffin cells are shown. Cells were stimulated by depolarising pulses to 0 mV for 15 ms (panel A), 50 ms (panel B) or 1 s (panel C). As shown, inactivation of the late current was more pronounced with the increasing duration of the depolarising pulse.

block of N channels by ω-conotoxin GVIA (Olivera et al., 1984), this toxin was removed from the superfusion solution at this point; however, nifedipine remained for the rest of the experiment and ω-agatoxin IVA (2 μM) was added to the nifedipine solution. Upon addition of ω-agatoxin IVA, I_{Ba} started a new decay phase, that developed slowly to reach a steady state inward current of only −0.05 nA. Washout of ω-agatoxin IVA did not allow current recovery (not shown). In 13 cells, the L/N component accounted for an average of 40% of I_{Ba}, and the P/Q component amounted to 60%. The frequency distribution histogram of Fig. 1B shows that, in more than 50% of cells, the fraction of the whole-cell current carried through P/Q channels accounted for more than 50%. Thus, this protocol allows the whole-cell current component carried by P/Q channels to be isolated from that carried by L- and N-subtypes of Ca^{2+} channels. The inset in Fig. 1A shows three original traces; the first was taken immediately before adding nifedipine plus ω-conotoxin GVIA (trace a, control current), the second immediately before adding ω-agatoxin IVA (trace b, current resistant to nifedipine plus ω-conotoxin GVIA), and the third one immediately before washing out ω-agatoxin IVA (trace c; only 5% of current remained unblocked). All three blockers decreased the amplitude of peak I_{Ba}, without causing inactivation of the current, a behaviour that differed from that of dotarizine (see below).

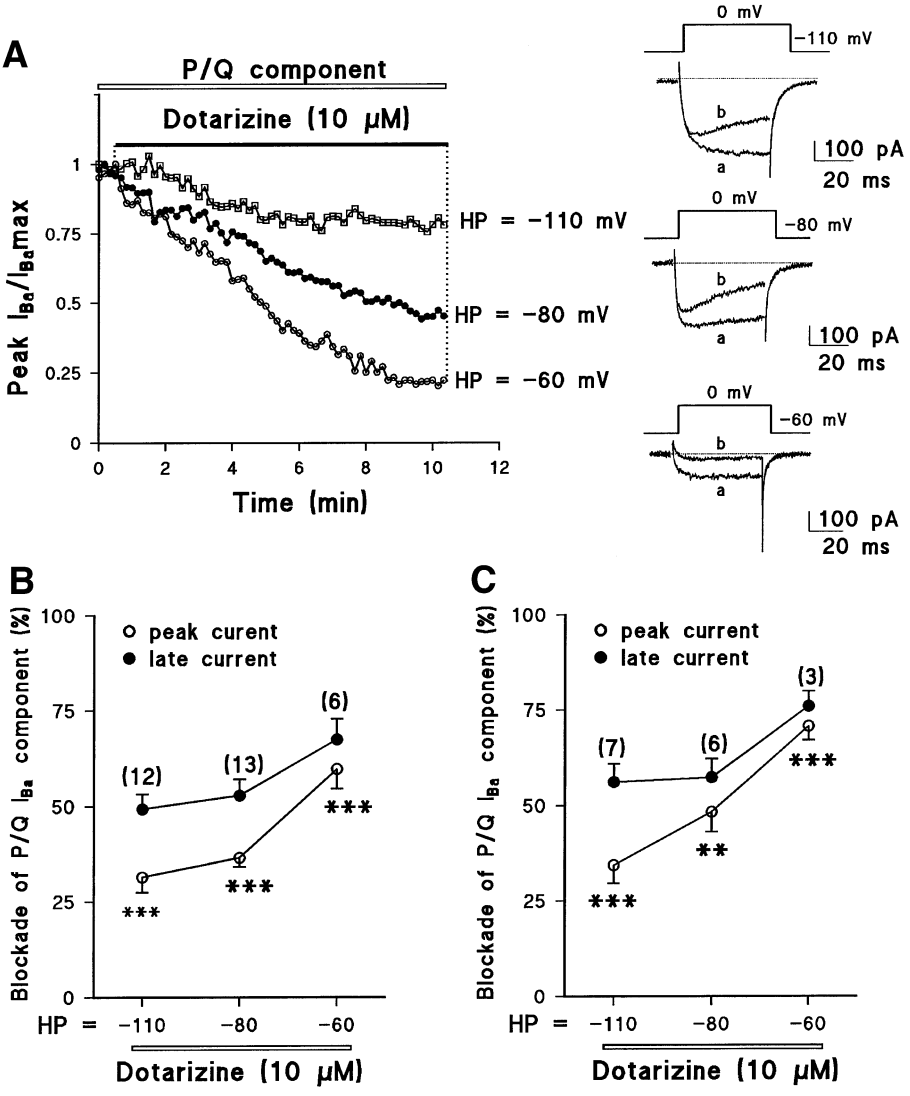

Fig. 3. Blockade by dotarizine of peak and late current through P/Q Ca^{2+} channels, at various holding potentials. A single, separate cell was used for each holding potential; each cell was treated with ω-conotoxin GVIA plus nifedipine, as in Fig. 1. The cells were voltage-clamped at holding potentials of −110, −80 or −60 mV; 50-ms test depolarising pulses to 0 mV were applied at 10-s intervals and dotarizine was applied during a 10-min period in all cases (top horizontal bar). Panel A shows the time course of the inhibition by dotarizine of I_{Ba}, in three cells with different holding potential; in the right part, typical current traces are shown for each holding potential. Panels B and C show averaged results for the inhibition of peak and late I_{Ba}, induced by dotarizine at the three holding potentials studied, after 5-min superfusion (panel B) or 10-min superfusion with dotarizine (panel C). Data are means ± S.E.M. for the number of cells shown in parentheses. $^{**}P<0.01$; $^{***}P<0.005$, paired *t*-test.

3.2. Blockade of the late P/Q Ca^{2+} channel current induced by dotarizine is a function of the length of the depolarising test pulse

In preliminary experiments, dotarizine (3–30 μM) seemed to promote the inactivation of I_{Ba} through P/Q channels, suggesting the possibility that dotarizine could block open P/Q channels. Thus, the idea was tested that dotarizine will block more effectively I_{Ba}, the longer is the depolarising pulse. Chromaffin cells were voltage-clamped at −80 mV and treated with ω-conotoxin GVIA plus nifedipine in the usual way, to isolate the P/Q channel currents. Currents were elicited by means of test depolarising pulses of increasing duration (15, 50 and 1000 ms).

Panel A of Fig. 2 shows original current traces obtained in a chromaffin cell stimulated by 15-ms depolarising pulses. With these short pulses, no time was allowed to cause inactivation of the current in the absence of dotarizine. Upon superfusion of dotarizine (10 μM), the peak and late I_{Ba} were gradually blocked in a parallel manner. This behaviour contrasts sharply with that seen with longer depolarising pulses (panels B and C of Fig. 2). With such longer pulses, a pronounced inactivation of I_{Ba} through P/Q

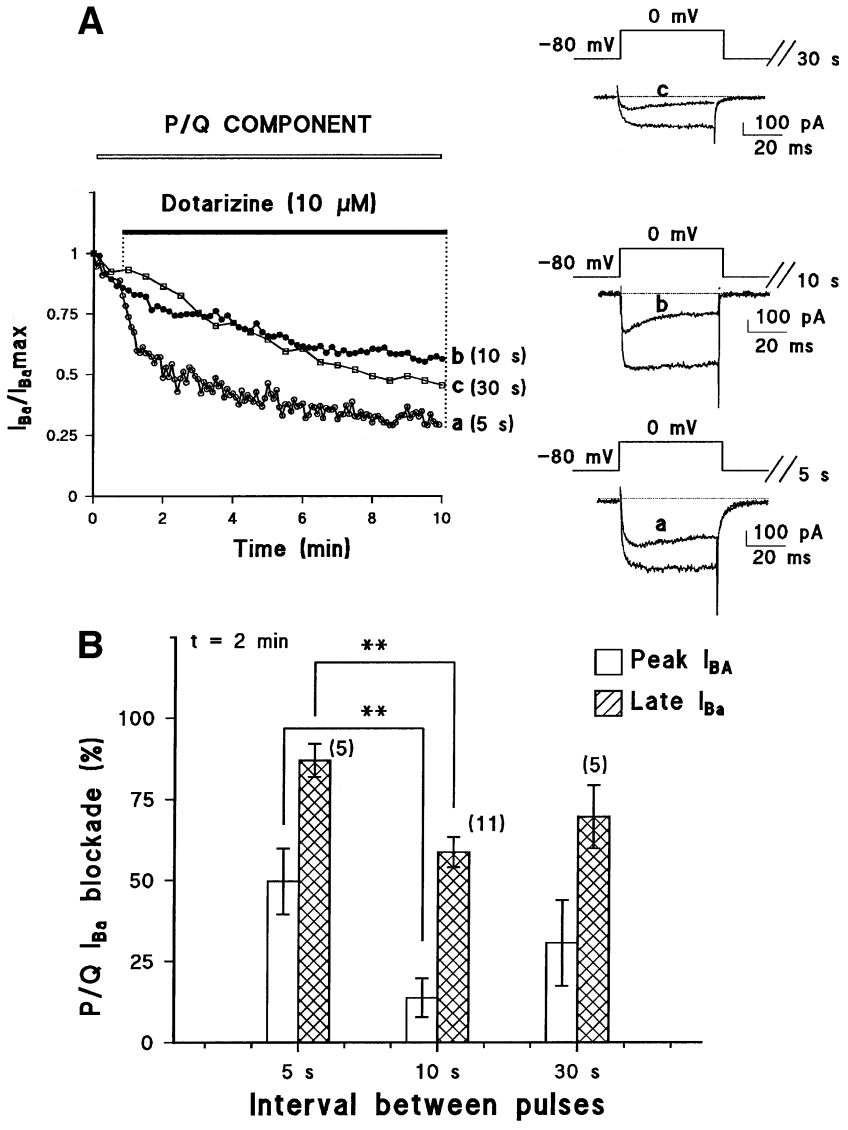

Fig. 4. Blockade by dotarizine of P/Q Ca^{2+} channel current depends on the frequency of application of test depolarising pulses. The cells were voltage-clamped at −80 mV; test depolarising pulses to 0 mV of 50-ms duration were applied at intervals of 5, 10 and 30 s. The cells were pretreated with ω-conotoxin GVIA plus nifedipine, as in Fig. 1, to isolate the P/Q Ca^{2+} channel current component. The cells were superfused continuously with the extracellular solution (10 mM Ba^{2+}) that contained dotarizine during the time period shown by the top horizontal bar. Panel A shows the time course of blockade by dotarizine of I_{Ba}, in three different cells stimulated with 50-ms depolarising pulses, at the intervals indicated in parentheses. Panel B shows averaged results for the percentage blockade induced by dotarizine on peak (white columns) and late current (black columns), following stimulation at intervals of 5, 10 or 30 s, after 2-min superfusion with the drug; they are means ± S.E.M. for the number of cells shown in parentheses on top of each bar. $^{**}P < 0.01$.

channels was observed, as reflected by a fast blockade of the late I_{Ba}, that amounted to as much as 80% after only 1 min of superfusion with 10 μM dotarizine, when 1-s depolarising pulses were applied.

3.3. Blockade by dotarizine of P/Q Ca^{2+} channels as a function of membrane potential

To test whether dotarizine caused a voltage-dependent blockade of P/Q Ca^{2+} channel current, the cells were voltage-clamped at −110, −80 or −60 mV, and treated with ω-conotoxin GVIA and nifedipine to isolate the P/Q current. Then, test depolarising pulses to 0 mV were applied at 10-s intervals from their respective holding potential. Dotarizine (10 μM) was added once the current had stabilised at each holding potential. These currents suffered no decay during a 10-min period, in the absence of the drug (not shown).

Fig. 3A shows the normalised time course of current through P/Q channels and its blockade by dotarizine (10 μM) at the various holding potentials tested. Dotarizine exhibited a clear voltage-dependence of its blocking effects of P/Q channels. Thus, at −110 mV, the peak current blockade amounted to only 23% of the initial current after 10-min superfusion of dotarizine; at −80 mV, the blockade amounted to 55% of the initial current, and at −60 mV to 78% (panel A). The current traces shown on the right part of panel A show the kinetic of inactivation of I_{Ba} after 10 min of dotarizine treatment; observe the pronounced inactivation of I_{Ba} in the presence of dotarizine (traces "b"), compared to control currents (traces "a"), at −110 and −80 mV. This current inactivation was not seen at −60 mV because the current blockade was very pronounced.

Panels B and C show pooled results from 3–13 cells. Note that the late current was inhibited more at depolarising potentials, probably because at more depolarising potentials, the current inactivated faster, even after 5-min (panel B) or 10-min superfusion with dotarizine (panel C).

3.4. Frequency-dependent blockade of P/Q channels induced by dotarizine

It is likely that the relaxation of I_{Ba} produced by dotarizine is due to an open-channel blockade; if so, we may predict that the higher the frequency of stimulation, the faster the blockade of P/Q channel current should be. The experiments of Fig. 4 were performed to test this possibility: in panel A, separate cells were stimulated with test depolarising pulses of 50-ms duration at 5-, 10- or 30-s intervals. Observe that blockade was faster, the shorter were the time intervals between depolarising pulses (5 s), the differences being more pronounced at the beginning of the superfusion period with dotarizine. No differences were observed between 10- and 30-s intervals. The original traces shown on the right of panel A show once more the kinetic differences of I_{Ba} before or during superfusion with dotarizine. Note the current inactivation in presence of the drug (traces a, b and c).

To better evaluate the differences between the time intervals studied, the blockade achieved after 2-min superfusion with dotarizine was plotted in Fig. 4B. When pulses were applied at 5-s intervals, the peak current was blocked by 49 ± 10% and the late current was blocked by 87 ± 5%. When pulses were applied at 10-s intervals, after 2-min superfusion with dotarizine, the peak current was blocked by only 13 ± 7% and the late current by 60 ± 5%. No

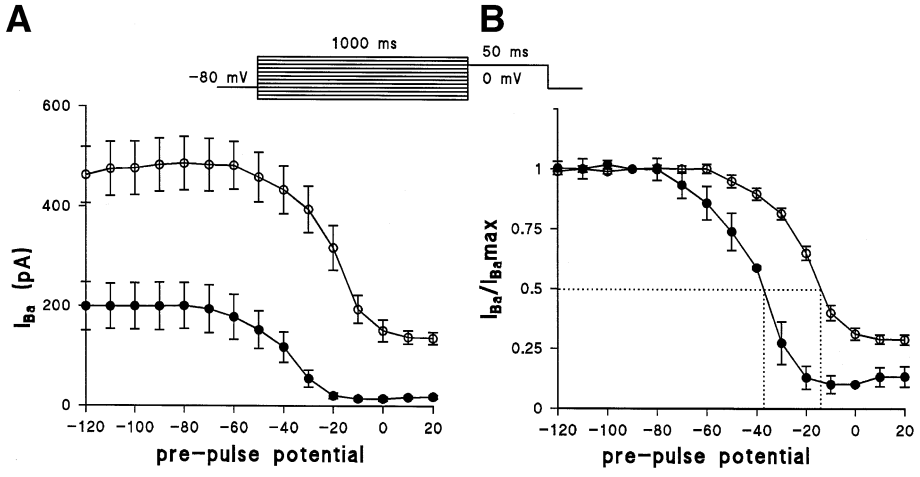

Fig. 5. Dotarizine shifts to the left the voltage-inactivation curve for P/Q channel currents. To isolate the P/Q channel currents, cells were treated with ω-conotoxin GVIA plus nifedipine, as in Fig. 1. Panel A shows the average peak current obtained after the application of pre-pulses at the different potentials indicated, obtained in the absence or in the presence of 10 μM dotarizine. The cells were voltage-clamped at −80 mV. Pre-pulses of 1000-ms duration, at the voltages shown in the abscissa, preceded the test depolarising pulses to 0 mV and 50-ms duration. Panel B shows normalised (I_{Ba}/I_{Ba}max) steady state inactivation curves obtained under both conditions. The voltage for half-inactivation ($V_{1/2}$) of I_{Ba} was −15 mV for control cells and −38 mV in cells treated with dotarizine. Data are means ± S.E.M. for the number of cells shown in parentheses.

significant differences were observed between 10- and 30-s intervals; however, the differences between the extent of blockade elicited by dotarizine in cells stimulated at 5-s intervals were significantly different from 10-s ($P<0.01$; panel B).

3.5. Dotarizine shifts the steady state inactivation of P/Q Ca^{2+} channels

To further characterize the mechanism involved in the dotarizine blockade of P/Q channels, steady state voltage-inactivation curves were performed in the absence and presence of 10 μM dotarizine, in cells voltage-clamped at −80 mV (Fig. 5). In these experiments, 1-s depolarising pre-pulses to different potentials were applied preceding the application of a 50-ms depolarising pulse to 0 mV. Fig. 5A shows the average steady state inactivation curve of seven cells both in the absence (open circles) and in the presence (solid circles) of dotarizine (10 μM). Superfusion with dotarizine produced a 30–40% blockade of peak current. Panel B shows the normalised currents (I_{Ba}/I_{Ba}max) obtained under both experimental conditions. Dotarizine decreased not only the magnitude of peak I_{Ba}, but also displaced to the left the steady state inactivation curve as well. In the absence of dotarizine, half-inactivation of P/Q channel current occurred at -15.8 ± 3.1 mV in 7 cells. Dotarizine shifted to the left the value of the pre-pulse voltage for half-inactivation of the current (-38.2 ± 5 mV in six cells; panel B).

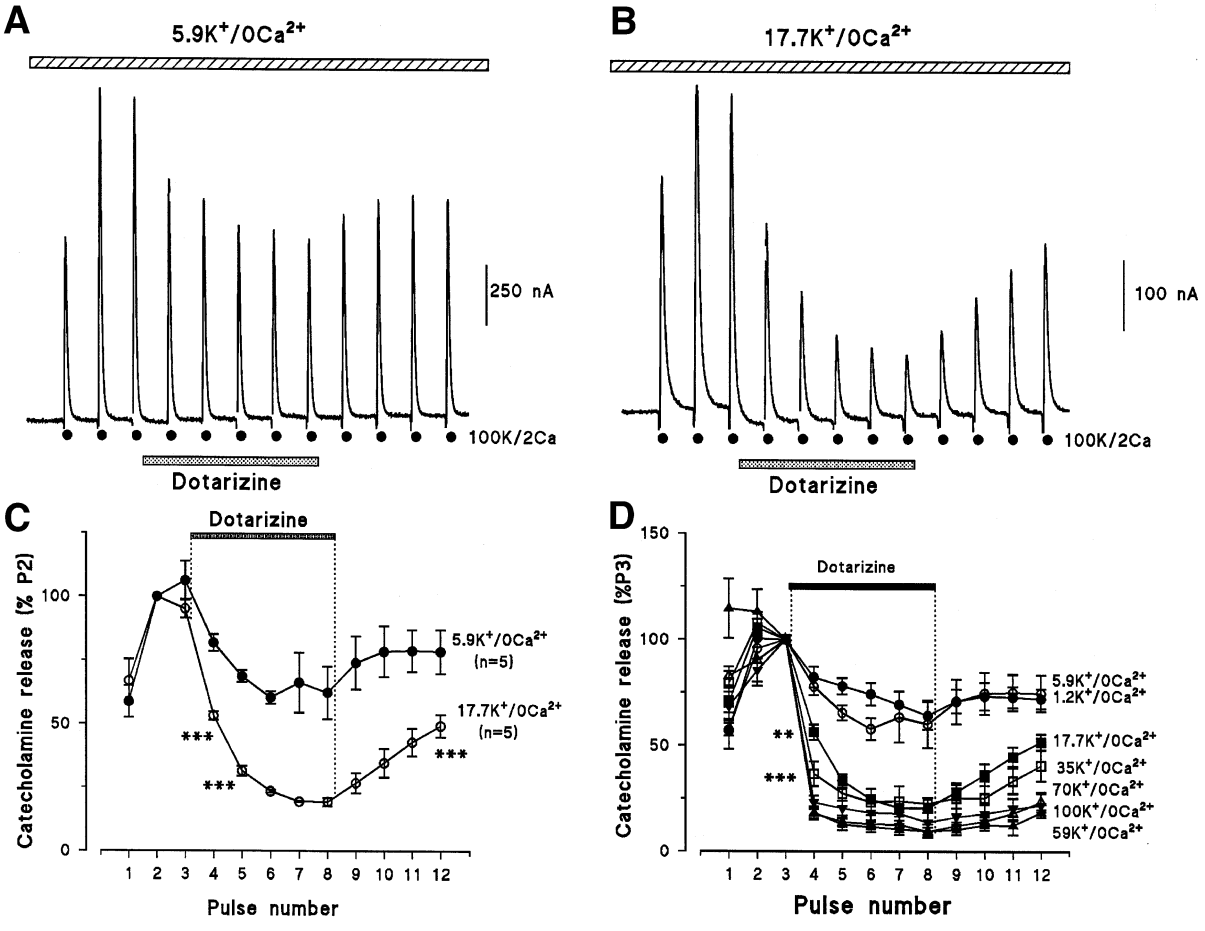

Fig. 6. Blockade by dotarizine of catecholamine release induced by short pulses of K^+ plus Ca^{2+}, in fast superfused chromaffin cells. After a stable baseline was obtained for secretion, the cells were intermittently stimulated at 2-min intervals to secrete catecholamines, with 2-s pulses of a solution containing 100 mM K^+ (with iso-osmotic reduction of Na^+) and 2 mM Ca^{2+} ($100K^+/2Ca^{2+}$). Panels A and B show the original spikes of secretion obtained in two prototype experiments. In panel A, cells (5×10^6) were continuously superfused with a nominal $0Ca^{2+}$ solution containing 5.9 mM K^+ ($5.9K^+/0Ca^{2+}$) and in panel B, cells were superfused with a nominal $0Ca^{2+}$ solution containing 17.7 mM K^+ ($17.7K^+/0Ca^{2+}$) as shown by the white horizontal bars. Dots at the foot of each spike show the $100K^+/2Ca^{2+}$ challenge. After the three initial challenges to get stable secretory spikes, dotarizine (3 μM) was given for a 10-min period during which five more $100K^+/2Ca^{2+}$ challenges were applied (black horizontal bar). Then, four additional $100K^+/2Ca^{2+}$ pulses were applied to test the recovery of the secretory response. Panel C shows the average values of the secretory spikes, normalised with respect to the catecholamines secreted in the second control pulse (P2). They are means ± S.E.M. for the number of cell batches from different cultures, shown in parentheses at the right of each graph. Panel D shows pooled results obtained from experiments performed with different K^+ concentrations (1.2, 5.9, 17.7, 35, 59, 70, 100 mM) in nominal $0Ca^{2+}$; stimulation of secretion was done with 2-s pulses of a $100K^+/2Ca^{2+}$ solution. Data are normalized with respect to the catecholamines secreted in the third control pulse (P3). $^{**}P<0.01$; $^{***}P<0.001$.

3.6. Effects of dotarizine on catecholamine release from chromaffin cells superfused with solutions of increasing depolarising strength

To find a functional correlate for the electrophysiological data, the effects of dotarizine (3 μM) on catecholamine release were studied. The idea was to test whether the voltage-dependent blockade of Ca^{2+} channel currents induced by dotarizine had a similar voltage-dependence for the block of secretion. To achieve this, cells were superfused with various Krebs-HEPES solutions lacking Ca^{2+} and containing increasing concentrations of K^+, referred to as nominal $0Ca^{2+}$ solutions of increasing depolarising strength ($1.2K^+/0Ca^{2+}$; $5.9K^+/0Ca^{2+}$; $17.7K^+/0Ca^{2+}$; etc). Then secretion was triggered by applying brief pulses (2-s) of a Krebs-HEPES solution containing 100 mM K^+ and 2 mM Ca^{2+} ($100K^+/2Ca^{2+}$). All alterations of $[K^+]_e$ were osmotically corrected for by reducing $[Na^+]_e$ in the appropriate concentration.

Fig. 6A shows the secretory spikes evoked by challenges with $100K^+/2Ca^{2+}$ in cells superfused with the more physiological concentration of K^+ in $0Ca^{2+}$ ($5.9K^+/0Ca^{2+}$). On the third challenge, secretion stabilised at around 1000 nA. Dotarizine induced a gradual blockade of secretion that reached about 35% after the fifth $100K^+/2Ca^{2+}$ pulse. The blockade of secretion developed much faster and was much greater when cells were superfused with a $17.7K^+/0Ca^{2+}$ solution (Fig. 6B). In fact, after only 2-min superfusion with 3 μM dotarizine, the blockade of secretion amounted to as much as 70%. The differences between $5.9K^+/0Ca^{2+}$ and $17.7K^+/0Ca^{2+}$ are seen more clearly in the averaged results shown in Fig. 6C. The maximum blockade achieved in $5.9K^+/0Ca^{2+}$ after 10-min superfusion with dotarizine amounted to $40 \pm 2.5\%$ ($n = 5$); on superfusion with $17K^+/0Ca^{2+}$, however, the blockade reached $81 \pm 1.6\%$. Panel D shows pooled results obtained from experiments performed with different K^+ concentrations (1.2, 5.9, 17.7, 35, 59, 70, 100 mM) in nominal $0Ca^{2+}$; stimulation of secretion was always done with 2-s pulses of a $100K^+/2Ca^{2+}$ solution. Note that the blockade exerted by dotarizine increased drastically even with mild depolarisations of chromaffin cells, i.e. 17.7 or 35 mM K^+ (in $0Ca^{2+}$). Stronger depolarisations caused little further increase of dotarizine-evoked blockade of secretion.

4. Discussion

The P/Q component of the whole-cell inward current through Ca^{2+} channels that accounted for 50–60% in bovine chromaffin cells was blocked by dotarizine in a time-dependent manner. What seemed more striking was the slow development of the blockade. In principle, the high lipophilicity of dotarizine (Lara et al., 1997) precludes slow access to its plasma membrane receptor on the P/Q Ca^{2+} channel. Being highly lipophilic, dotarizine should easily penetrate the lipid bilayer and accumulate at the plasma membrane in few seconds. Thus, to explain the delayed blocking of the current, one has to look at the kinetics of the ion channel itself. A given conformation may be required to allow access and binding of dotarizine to its receptor site on the P/Q channel. The following arguments favour the hypothesis that dotarizine blocks open Ca^{2+} channels to promote their rapid closing.

For instance, the longer the duration of the depolarising test pulse, the greater the blockade of the late current. It is interesting that the peak I_{Ba} was similarly inhibited by dotarizine with short (15 or 50 ms) or long depolarising pulses (1000 ms); and that the late I_{Ba} was blocked, the more the longer was the depolarising pulse. This can be interpreted as follows. Early in a long pulse, all channels are open; thus, dotarizine binds to its receptor, closing the channels gradually and promoting inactivation of the current. With very short pulses, there is not enough time for dotarizine to act. Thus, the longer the pulse, the greater is the binding of the compound to open channels, and the higher their blockade. This explains why dotarizine causes a much stronger blockade of the late I_{Ba} than of the peak I_{Ba}; it also explains why the molecule causes a greater blockade of I_{Ba} at faster stimulation frequencies: the higher the frequency, the longer P/Q channels are in their open state and the better is the access of dotarizine to its receptor.

Another interesting kinetic feature is the voltage-dependence of the blockade. The greater blockade seen when cells were held at −60 mV, as compared to −80 and −110 mV, clearly suggests that dotarizine binds to its receptor site better at more depolarising potentials. The marked shift to the left (25 mV) of the voltage-inactivation curve for P/Q channels caused by dotarizine, also indicates that dotarizine causes a greater current blockade at more depolarising potentials. This means that the drug favours the inactivation of P/Q channels.

It is interesting that dotarizine and ω-agatoxin IVA are blocking the same fraction of the whole-cell inward Ca^{2+} channel current. This suggests that, like ω-agatoxin IVA, dotarizine blocks the P/Q channels of chromaffin cells. It is even more interesting that the mechanism of the blockade differs for the two compounds. Thus, in contrast to dotarizine, ω-agatoxin IVA blocked the P/Q channel current in a parallel manner, and did not provoke its inactivation; this parallelism occurred with short as well as with long depolarising pulses (not shown; see Albillos et al., 1993).

P/Q Ca^{2+} channels are implicated in the control of the Ca^{2+}-dependent exocytotic release of neurotransmitters in various brain areas (Wheeler et al., 1994, 1995), as well as in the release of catecholamines from chromaffin cells (López et al., 1994; Lara et al., 1998). Thus, it was important to ascertain whether the mechanism of blockade of P/Q channels by dotarizine had functional relevance for the control of exocytosis. At concentrations similar to those blocking P/Q channels, we have demonstrated here

that dotarizine inhibits the release of catecholamines triggered by short K^+ pulses. Since this secretory signal is due to P/Q channel activation (López et al., 1994), it seems that the blockade of catecholamine release now seen was due, at least partially, to inhibition of P/Q channels. What seems the most interesting is that the blockade of secretion induced by dotarizine is much faster and more pronounced in depolarised cells. This might have physiopathological and therapeutic implications for the potential clinical use of dotarizine in patients with chronic migraine.

Clinical trials have shown that dotarizine is efficacious to prevent migraine attacks in migraineur patients (Horga et al., 1996). In the physiopathology of a migraine crisis, vascular as well as neurogenic components are being considered (Humphrey et al., 1991; Martins et al., 1993; Lance, 1993; Williamson et al., 1996). The release of vasoactive neuropeptide transmitters from trigeminal nerve terminals is considered to be an essential step in the crisis of migraine. If this Ca^{2+}-dependent, exocytotic release of neuropeptides was controlled by extracellular Ca^{2+} entering through P/Q Ca^{2+} channels, then it follows that by blocking such channels and Ca^{2+} entry, dotarizine could prevent the release of vasoactive neurotransmitters and the triggering of a migraine attack. It is interesting that focal cerebral ischemia has been described to occur during migraine attacks (Lauritzen et al., 1983); this could lead to neuronal tissue depolarisation. Since dotarizine blocks exocytosis much better and faster in depolarised cells, it follows that, in depolarised brain tissues of migraineurs, dotarizine could gain access more readily to P/Q channels, to efficiently block the release of trigeminal vasoactive neuropeptides to abort a migraine crisis. In human volunteers, the therapeutic doses of oral dotarizine produce peak plasma levels of 0.5 μM (data on file, Ferrer International, Barcelona, Spain). This concentration is about eight-fold lower than the in vitro IC_{50} of dotarizine to block I_{Ba}, and six-fold lower than the concentration of dotarizine to block exocytosis. However, the high lipophilicity of dotarizine may lead to greater concentrations in target cells.

In conclusion, dotarizine efficiently blocks the neuronal P/Q type of Ca^{2+} channels in a voltage-, time- and frequency-dependent manner. Exocytotic catecholamine release is also blocked in a voltage-dependent manner. This, together with its vascular effects (Ruiz-Nuño et al., 2001), might help understand the mechanism involved in the beneficial effects of dotarizine to prevent migraine attacks.

Acknowledgements

Supported by grants from DGICYT (No. PM99-0004 to LG and No. PM99-0005 to AGG), Programa Grupos Estratégicos III PRICIT de la Comunidad Autónoma de Madrid, FIS (No. 01/183 to AGG) and Fundación Teófilo Hernando, Spain. We thank Mr. Ricardo de Pascual for the preparation of excellent cell cultures.

References

Albillos, A.G., García, A.G., Gandía, L., 1993. ω-Agatoxin-IVA-sensitive calcium channels in bovine chromaffin cells. FEBS Lett. 336, 259–262.

Albillos, A., García, A.G., Olivera, B., Gandía, L., 1996. Re-evaluation of the P/Q Ca^{2+} channel components of Ba^{2+} currents in bovine chromaffin cells superfused with solutions containing low and high Ba^{2+} concentrations. Pflügers Arch. Eur. J. Physiol. 432, 1030–1038.

Borges, R., Sala, F., García, A.G., 1986. Continuous monitoring of catecholamine release from perfused cat adrenals. J. Neurosci. Methods 16, 389–400.

Brasó, A., Martínez, L., Planas, J.M., Cartheuser, C.F., Sacristán, A., Ortiz, A., 1996. Pharmacological profile and actions of dotarizine as a prophylactic antimigraine drug. J. Neurol. 243 (Suppl. 2), 6.

Fenwick, E.M., Marty, A., Neher, E., 1982. Sodium and calcium currents in bovine chromaffin cells. J. Physiol. 331, 599–635.

Galiano, L., Matias-Guiu, J., Horga, J.F., Martín, R., Falip, R., Montiel, I., 1993. Dotarizine: a double-blind trial in prophylactic treatment of migraine. Cephalalgia 13 (Suppl. 13), 251.

Gandía, L., Lara, B., Imperial, J., Villarroya, M., Albillos, A., Maroto, R., García, A.G., Olivera, B.M., 1997. Analogies and differences between ω-conotoxins MVIIC and MVIID: binding sites and functions in bovine chromaffin cells. Pflügers Arch. Eur. J. Physiol. 435, 55–64.

García, A.G., Gandía, L., López, M.G., Montiel, C., 2000. Calcium channels for exocytosis: functional modulation with toxins. In: Botana, L. (Ed.), Seafood and Fresh Water Toxins: Pharmacology, Physiology and Detection. Marcel Decker, New York, pp. 91–124.

Hamill, O.P., Marty, A., Neher, E., Sakmann, B., Sigworth, F.J., 1981. Improved path-clamp techniques for high resolution current recording from cells and cell-free membrane patches. Pflügers Arch. Eur. J. Physiol. 391, 85–100.

Horga, J.F., Matías-Guiu, J., Castillo, J., Laínez, J.M., Hernández, M., Faura, C.C., 1996. Comparison of dotarizine and pizotifen in prophylactic treatment of migraine: a crossover double-blind multicentre study. In: Congress Abstracts 8th World Congress on Pain, Vancouver, Canada, p. 501.

Humphrey, P.P., Feniuk, W., Marriott, A.S., Tanner, R.J., Jackson, M.R., Tucker, M.L., 1991. Preclinical studies on the anti-migraine drug, sumatriptan. Eur. Neurol. 31, 282–290.

Lance, J.W., 1993. Current concepts of migraine pathogenesis. Neurology 43, S11–S15.

Lara, B., Gandía, L., Torres, A., Olivares, R., Martínez-Sierra, R., García, A.G., López, M.G., 1997. Wide-spectrum Ca^{2+} channel antagonists: lipophilicity, inhibition and recovery of secretion in chromaffin cells. Eur. J. Pharmacol. 325, 109–119.

Lara, B., Gandía, L., Martínez-Sierra, R., Torres, A., García, A.G., 1998. Q-type Ca^{2+} channels are located closer to secretory sites than L-type channels: functional evidence in chromaffin cells. Pflügers Arch. Eur. J. Physiol. 435, 472–478.

Lauritzen, M., Skyhoj Olsen, T., Lassen, N.A., Paulson, O.B., 1983. Changes in regional cerebral blood flow during the course of classic migraine attacks. Ann. Neurol. 41, 633–641.

Livet, B.G., 1984. Adrenal medullary chromaffin cells in vitro. Physiol. Rev. 64, 1103–1161.

López, M.G., Villarroya, M., Lara, B., Martínez-Sierra, R., Albillos, A., García, A.G., Gandía, L., 1994. Q- and L-type Ca^{2+} channels dominate the control of secretion in bovine chromaffin cells. FEBS Lett. 349, 331–337.

Martins, I.P., Baeta, E., Paiva, T., Campos, J., Gomes, L., 1993. Headaches during intracranial endovascular procedures: a possible model of vascular headache. Headache 33, 227–233.

Montiel, C., Herrero, C.J., García-Palomero, E., Renart, J., García, A.G., Lomax, R.B., 1997. Serotonergic effects of dotarizine in coronary artery and in oocytes expressing 5-HT_2 receptors. Eur. J. Pharmacol. 332, 183–193.

Moro, M.A., López, M.G., Gandía, L., Michelena, P., García, A.G., 1990. Separation of living adrenaline- and noradrenaline-containing cells from bovine adrenal medullae. Anal. Biochem. 185, 243–248.

Novalbos, J.M., Abad-Santos, F., Zapater, P., Cano-Abad, M.F., Moradiellos, J., Sánchez-García, P., García, A.G., 1998. Effects of dotarizine and flunarizine on chromaffin cell viability and cytosolic Ca^{2+}. Eur. J. Pharmacol. 366, 309–317.

Novalbos, J.M., Abad-Santos, F., Zapater, P., Alvarez, J., Alonso, M.T., Montero, M., García, A.G., 1999. Novel antimigraineur dotarizine releases calcium from caffeine-sensitive calcium stores of chromaffin cells. Br. J. Pharmacol. 128, 621–626.

Olivera, B.M., Mcintosh, J.M., Cruz, L.J., Luque, F.A., Gray, W.R., 1984. Purification and sequence of a presynaptic peptide toxin from *Conus geographus* venom. Biochemistry 23, 5087–5090.

Olivera, B.M., Miljanich, G., Ramachandran, J., Adams, M., 1994. Calcium channel diversity and neurotransmitter release: the ω-conotoxin and ω-agatoxins. Ann. Rev. Biochem. 63, 823–867.

Ophoff, R.A., Terwindt, G.M., Vergouwe, M.N., Van Eijk, R., Oefner, P.J., Hoffman, S.M., Lamerdin, J.E., Mohrenweiser, H.W., Bulman, D.E., Ferrari, M., Haan, J., Lindhout, D., Van Ommen, G.J., Hofker, M.H., Ferrari, M.D., Frants, R.R., 1996. Familial hemiplegic migraine and episodic ataxia type-2 are caused by mutations in the Ca^{2+} channel gene CACNL1A4. Cell 87, 543–552.

Ruiz-Nuño, A., Villarroya, M., Cano-Abad, M.F., Rosado, A., López, M.G., García, A.G., 2001. Mechanism of blockade by the novel migraine prophylactic agent, dotarizine, of various brain and peripheral vessel contractility. Eur. J. Pharmacol. 411, 289–299.

Tejerina, T., Chulia, T., González, P., 1993. Effects of dotarizine on $^{45}Ca^{2+}$ movements and contractile responses in vascular smooth muscle. Eur. J. Pharmacol. 239, 75–81.

Villarroya, M., Gandía, L., Lara, B., Albillos, A., López, M.G., García, A.G., 1995. Dotarizine versus flunarizine as calcium antagonists in chromaffin cells. Br. J. Pharmacol. 114, 369–376.

Wheeler, D.B., Randall, A., Tsien, R.W., 1994. Roles of N- and Q-type Ca^{2+} channels in supporting hippocampal transmission. Science 264, 107–111.

Wheeler, D.B., Randall, A., Sather, W.A., Tsien, R.W., 1995. Neuronal calcium channels encoded by the alpha 1A subunits and their contribution to excitatory synaptic transmission in the CNS. Prog. Brain Res. 105, 65–78.

Williamson, J.W., Friedman, D.B., Mitchell, J.H., Secher, N.H., Friberg, L., 1996. Mechanisms regulating regional cerebral activation during dynamic handgrip in humans. J. Appl. Physiol. 81, 1884–1890.